Optoelectronic properties and electronic structure of YCuOSe

Kazushige Ueda[a)]
Department of Materials Science, Faculty of Engineering, Kyushu Institute of Technology, 1-1 Sensui, Tobata, Kitakyushu, Fukuoka 804-8550, Japan

Kouhei Takafuji, Hiroshi Yanagi, Toshio Kamiya,[b)] and Hideo Hosono[b),c)]
Materials and Structures Laboratory, Tokyo Institute of Technology, Mailbox R3-1, 4259 Nagatsuta, Midori, Yokohama 226-8503, Japan

Hidenori Hiramatsu and Masahiro Hirano
ERATO-SORST, Japan Science and Technology Agency (JST), in Frontier Collaborative Research Center (FCRC), Tokyo Institute of Technology, Mailbox S2-13, 4259 Nagatsuta, Midori, Yokohama 226-8503, Japan

Noriaki Hamada
Department of Physics, Faculty of Science and Technology, Tokyo University of Science, 2641 Yamazaki, Noda, Chiba 278-8510, Japan

(Received 12 September 2007; accepted 25 October 2007; published online 10 December 2007)

YCuOSe was prepared by solid-state reaction, and its wide gap semiconducting properties were examined. The single phase of YCuOSe was obtained in a limited temperature range around 750 °C and decomposed into Y_2O_2Se and Cu_2Se at higher temperatures. The obtained YCuOSe sample showed a *p*-type semiconducting behavior with the electrical conductivity of 1.4×10^{-1} S cm^{-1} at room temperature. The band gap of YCuOSe was estimated to be 2.58 eV, which is much smaller than that of LaCuOSe (2.82 eV). The electronic structure of YCuOSe was investigated by ultraviolet photoemission spectroscopy and energy band calculations to understand the differences in the electronic structures between LnCuOSe (Ln=La, Y). It was found that the Cu–Cu distance rather than the Cu–Se distance influences the electronic structures, and the smaller band gap of YCuOSe is attributed to the downshift of the Cu 4*s* energy level due to the smaller Cu–Cu distance and the consequent larger Cu–Cu interaction in YCuOSe. © *2007 American Institute of Physics*. [DOI: 10.1063/1.2821763]

INTRODUCTION

LaCuOS, a layered compound with a large band gap of 3.1 eV, is composed of $(La_2O_2)^{2+}$ and $(Cu_2S_2)^{2-}$ layers[1] and exhibits transparent *p*-type semiconducting properties and excitonic emission at room temperature.[2] Because of its unique optical and electrical properties, a number of studies have been reported from scientific and technological viewpoints.[3–10] Another important feature of this material is that there are many analogous compounds that have the same crystal structures as LaCuOS; each element can be substituted by another element with the same valence;[11–15] in addition, even each layer such as a $(La_2O_2)^{2+}$ or $(Cu_2S_2)^{2-}$ layer can be replaced by another layer such as a $(Ba_2F_2)^{2+}$ or $(Zn_2P_2)^{2-}$ layer with the same nominal charge.[16–19] These many analogous compounds bring about a wide variety of optical and electrical properties such as large third-order optical nonlinearity of LaCuOSe (Ref. 5) and superconductivity of LaFeOP.[20]

In the optoelectronic device application of LaCuOS or its analogs, we recently demonstrated room-temperature operation of a light-emitting diode and observed blue light emission from *p*-type LaCuOSe.[21] However, materials with the band gaps much wider than LaCuOCh (Ch=S, Se) are required to operate the devices in the ultraviolet region. Since our previous studies revealed that the $(Cu_2Ch_2)^{2-}$ (Ch=S, Se and Te) layer is essential for *p*-type semiconducting properties,[2,3] it would be reasonable to alter the $(La_2O_2)^{2+}$ layer to control the band gap in the layered compounds. We anticipated that replacing the $(La_2O_2)^{2+}$ layer with a $(Ba_2F_2)^{2+}$ or $(Y_2O_2)^{2+}$ layer would be effective to widen the band gaps because both BaF_2 (E_g=10.5 eV) and Y_2O_3 (6.1 eV) have wider band gaps than La_2O_3 (5.5 eV). Although it is reported that the band gap of BaCuFS is reported to be 3.25 eV,[22] that of YCuOS is unknown because the phase of YCuOS has not been prepared yet by a conventional solid-state reaction, in contrast to YCuOSe.[15]

In the series of LnCuOS (Ln=La, Pr and Nd), the band gap decreases as the atomic number of the lanthanide ions increases.[23] Similar band gap narrowing occurs in the series of LaCuOCh (Ch=S, Se, and Te). The changes of the band gap in LaCuOCh can be basically understood from the energy levels of the Ch ions because the Ch *p* orbitals form the top of the valence band (VB) with Cu 3*d* orbitals and influence the band gap directly.[24] On the other hand, the atomic orbitals of each lanthanide ion do not affect the band gap straightforward, and accordingly the origin of the band gap variation in LnCuOS is not the same with that in LaCuOCh. In this study, basic optical properties of YCuOSe were ex-

[a)]Electronic mail: kueda@che.kyutech.ac.jp.
[b)]Also at ERATO-SORST, JST, Japan.
[c)]Also at FCRC, Tokyo Institute of Technology, Japan.

amined as well as its electrical transport properties, and these properties were compared with those of LnCuOCh (Ln=La, Pr, and Nd; Ch=S,Se). In addition, ultraviolet photoemission spectroscopy (UPS) measurements and energy band calculations were carried out to understand the variation of band gaps in these oxychalcogenide materials.

EXPERIMENTS

Cu_2Se, Y_2Se_3, and Y_2O_3 were used as starting materials for YCuOSe. Cu_2Se and Y_2Se_3 were prepared in advance using Cu metal or Y metal and Se by heating them at 300 °C for 12 h in evacuated silica glass tubes. The starting materials of Cu_2Se, Y_2Se_3, and Y_2O_3 were mixed and disked by a cold isostatic press. The disks of YCuOSe samples were obtained by heating the pressed disks at 700, 750, or 900 °C for 12 h in evacuated silica glass tubes. After grinding the disks, the purity of the powdered samples was examined by power x-ray diffraction (XRD) measurements. The crystal structure of YCuOSe was analyzed by the Rietveld method using the RIETAN-2000 code.[25]

Electrical conductivities, Seebeck coefficients, diffuse reflectance, and photoluminescence (PL) spectra were measured using the disk or powder samples to examine their basic optical and electrical properties. Electrical conductivities were measured in the temperature range from RT to 10 K. The carrier polarity was examined from the sign of the Seebeck coefficients. Band gaps were estimated approximately from the absorption edges observed in the diffuse reflection spectra. The band edge emission was examined in the PL measurements using the 4ω of a Nd:YAG (yttrium aluminum garnet) laser as an excitation source.

UPS measurements were carried out along with the first-principles full-potential linearized augmented plane-wave (FLAPW) energy band calculations to understand the electronic structure of YCuOSe. The lines of He I (21.2 eV) or He II (40.8 eV) from a discharged lamp were used as excitation sources in the UPS measurements. The FLAPW band calculations by the ABCAP code were conducted using the crystal structural parameters obtained by the Rietveld analysis. The details of the UPS measurements and band calculations are reported elsewhere.[24]

RESULTS

Sample preparation and XRD analysis

The XRD patterns of the samples heated at 700, 750, or 900 °C are shown in Fig. 1. The starting materials of Cu_2Se and Y_2O_3 were remained in the sample heated at 700 °C, indicating that 700 °C is not high enough to complete the reaction to obtain a single-phase YCuOSe. On the other hand, the XRD pattern for the sample heated at 900 °C shows that the sample is almost decomposed into Y_2O_2Se and Cu_2Se. After all, the single-phase YCuOSe was obtained by heating samples at 750 °C for 12 h. This narrow formation temperature range for the single-phase YCuOSe is a contrast to those for LaCuOSe and LaCuOS, which are stable even at 1000 °C. This result suggests that YCuOSe is not as thermally stable as LaCuOS and LaCuOSe and would be related to the fact that its oxysulfide, YCuOS, has not been synthesized yet.

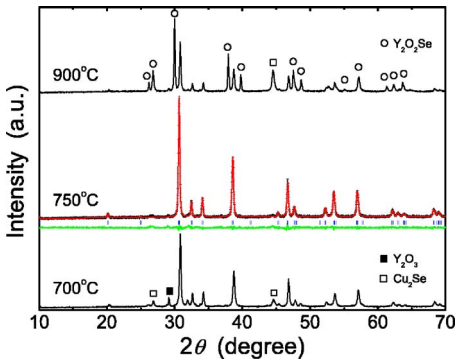

FIG. 1. (Color online) Powder XRD patterns for the samples heated at 700, 750, and 900 °C. For the 750 °C-heated sample, the observed pattern (+) and calculated pattern (solid line) are shown. The vertical bars and the line beneath the patterns exhibit the position of Bragg reflections and the difference of the patterns, respectively.

The crystal structural parameters of YCuOSe were refined by the Rietveld analysis. The obtained results are listed in Tables I(a) and I(b). To understand the structural differences among LnCuOCh (Ln=La,Y; Ch=S,Se), several interatomic distances are listed in Table II and shown in Fig. 2 along with the sum of the ion radii.[26] The Ln–O and Ln–Ch distances largely deviate from the sums of the ion radii. The shorter Ln–O distances and longer Ln–Ch distances of the measured values lead to the layered structures of LnCuOCh composed of $(Ln_2O_2)^{2+}$ oxide and $(Cu_2Ch_2)^{2+}$ chalcogenide layers. Both the Ln–O and Ln–Ch distances, as well as the lattice parameters, in YCuOSe are the smallest among LnCuOCh (Ln=La,Y; Ch=S,Se) because the radius of a Y ion (r_i=1.02 Å for sixfold coordination) is smaller than that of a La ion (r_i=1.16 Å). However, in spite of the smaller lattice parameters in YCuOSe than in LaCuOSe, the Cu–Se distances in YCuOSe are almost the same as that in LaCuOSe, varying the angles of ∠Se–Cu–Se. In contrast to the Cu–Ch distances, the Cu–Cu distances, which are solely determined by the *a*-axis length, obviously become smaller in YCuOSe than in LaCuOSe.

Electrical and optical properties

The temperature dependence of electrical conductivities for YCuOSe is shown in Fig. 3 along with those for LaCuOSe and LaCuOS. YCuOSe shows semiconducting behavior near room temperature and degenerate semiconducting behavior at low temperatures. The electrical conductivity of YCuOSe, which is higher than those of LaCuOSe or LaCuOS, is probably due to the higher density of hole carriers generated from defects such as Cu vacancies. The electrical conductivities and Seebeck coefficients at room temperature are summarized in the inset of Figure 3. The Seebeck coefficients are all positive, indicating that all the samples are *p*-type conductors.

The diffuse reflectance spectra and PL spectra of YCuOSe, LaCuOSe, and LaCuOS are shown in Fig. 4. The diffuse reflectances drop at 395 nm for LaCuOS, at 440 nm for

TABLE I. (a) Summary of refinement data and lattice parameters of YCuOSe. (b) Site occupancy, atomic positions, and isotropic thermal parameters.

(a)

Formula	YCuOSe
Space group	$P4/nmm$
a (Å)	3.8789(1)
c (Å)	8.7311(5)
V_{cell} (Å^3)	131.37(1)
Z	2
R_p	5.50
R_{wp}	7.37
R_e	6.14
S	1.20

(b)

	WN	g	x	y	z	B (Å^2)
Y	2c	1.0	1/4	1/4	0.1269(8)	0.2(3)
Cu	2b	1.0	1/4	3/4	1/2	1.5(5)
S	2c	1.0	1/4	1/4	0.6837(8)	0.2(3)
O	2a	1.0	1/4	3/4	0	0.0(1)

LaCuOSe, and at 480 nm for YCuOSe because of their fundamental absorption. Therefore, the substitution of Y for La causes a redshift of the absorption edge and the band gap of YCuOSe was estimated to be 2.58 eV. The band gaps of LnCuOCh and Ln_2O_3 (Ref. 27) are summarized in Table II. In the PL spectra, a sharp band edge emission was observed in YCuOSe at room temperature, as observed in LaCuOSe and LaCuOS. The observation of the band edge emission demonstrates that the band gap of YCuOSe is a direct-allowed-transition type similar to LaCuOCh and the PL is assigned to room-temperature stable excitons.

UPS spectra and electronic structures

The UPS spectra of YCuOSe, LaCuOSe, and LaCuOS are shown in Fig. 5. YCuOSe clearly shows a Cu–Se hybridized band at the top part of the VB as observed in LaCuOSe and LaCuOS. The vertical bars at ~2 eV indicate the bottoms of the Cu–Se hybridized bands and those at ~7–8 eV the bottoms of the VB. Because these materials are all p-type conductors, the Fermi energies, which are at the zero binding energy, are located at the top of the VB. Therefore, the bandwidths of the Cu–Se hybridized band or VB in each compound are approximately evaluated from the energy differences between the Fermi energy and the energy positions of the vertical bars. It is found from the UPS spectra that the bandwidths of the Cu–Se hybridized band are almost the same among YCuOSe, LaCuOSe, and LaCuOS, but the VB width of YCuOSe is larger than those of LaCuOSe and LaCuOS.

Figure 6 shows the energy band structures of YCuOSe, LaCuOSe, and LaCuOS. The energy of the VB maximum is aligned to zero in the energy scale. The band structures reveal that the band gap of YCuOSe is a direct-transition type and its value is the smallest among these compounds. Although the band calculation based on local density approximation usually underestimates the values of band gap, these results are consistent with the relative values of the band gaps in LnCuOCh (Ln=La, Y and Ch=S, Se) and the observation of the band edge emission. The Cu 3d-Se 4p hybridized band in each compound is mainly composed of four bands in the energy range from 0.0 to −1.5 eV, and the bandwidth of the hybridized band is almost the same among YCuOSe, LaCuOSe, and LaCuOS. On the other hand, the energy of the bottom of the VB in YCuOSe is different from those in LaCuOSe and LaCuOS, resulting in the largest VB width in YCuOSe. These bandwidths of the Cu 3d-Se 4p hybridized band and VB obtained by the band calculations are in good agreement with the VB structure observed in the UPS spectra.

DISCUSSION

Band gap of YCuOSe compared with LnCuOCh (Ln =La, Pr, Nd and Ch=S, Se)

TABLE II. Lattice parameters, interatomic distances, and energy gaps of LnCuOCh (Ln=La,Pr,Nd,Y; Ch=S,Se).

Substance LnCuOCh	Lattice parameters (Å)		Atomic distances (Å)			E_g (eV)	
	a	c	Ln–O	Cu–Ch	Cu–Cu	LnCuOCh	Ln_2O_3
LaCuOS	3.996	8.517	2.362	2.428	2.826	3.14	5.5
PrCuOS	3.941	8.438	2.33	2.42	2.787	3.03	4.6
NdCuOS	3.92	8.428	2.325	2.406	2.772	2.98	4.4
LaCuOSe	4.067	8.798	2.377	2.523	2.876	2.82	5.5
YCuOSe	3.879	8.731	2.234	2.517	2.743	2.58	6.1

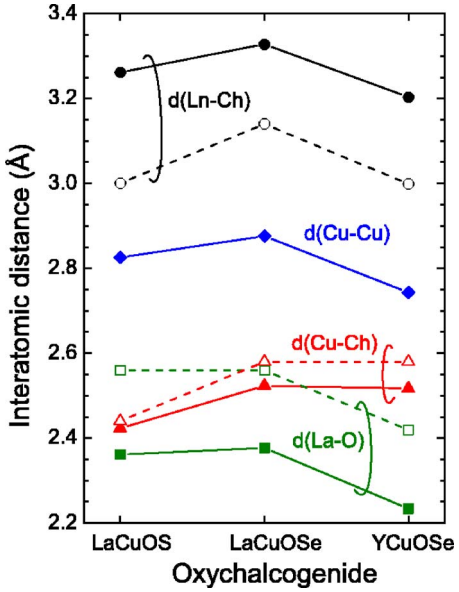

FIG. 2. (Color online) Measured interatomic distances (closed symbols) in LnCuOCh (Ln=La,Y; Ch=S,Se) along with the sum of ion radii of ion pairs (open symbols); Ln–O (squares), Ln–Ch (circles), Cu–Ch (triangles), and Cu–Cu (diamonds).

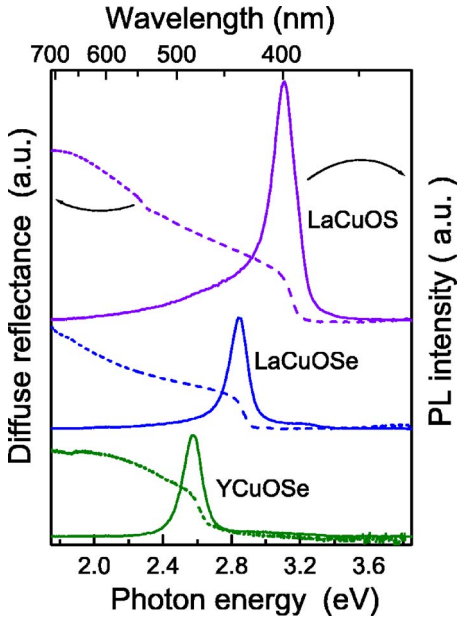

FIG. 4. (Color online) Diffuse reflectance spectra (dashed line) and PL spectra (solid line) of LaCuOCh (Ln=La,Y; Ch=S,Se).

The band gaps of the simple oxides, Ln_2O_3, vary in a wide range as large as 1 eV when the lanthanide ion is changed from La to Nd as summarized in Table II. The band gaps of LnCuOS (Ln=La,Pr,Nd) also decrease slightly as La is substituted with Pr or Nd. In the comparison between La and Y, the band gap of Y_2O_3 is larger than that of La_2O_3 by 0.5 eV; however, the band gap of YCuOSe is much smaller than that of LaCuOSe. Therefore, the variation of the band gaps in Ln_2O_3 seems to have no correlation with those in LnCuOCh. Namely, it is considered that the species of Ln ions (Ln=La,Pr,Nd,Y) do not influence the band gaps of LnCuOCh directly.

The lattice parameters, both *a* and *c*, decrease due to the lanthanide contraction when the lanthanide ion varies from La to Nd in LnCuOS (Ln=La,Pr,Nd). In LnCuOSe (Ln =La,Y), the lattice parameters also decrease when La ions are substituted by Y ions. In both LnCuOS and LnCuOSe, their band gaps decrease as their lattice parameters decreases, indicating that the variation of the band gaps in LnCuOCh depends on the size of Ln ions rather than the energy levels of the Ln-related atomic orbitals.

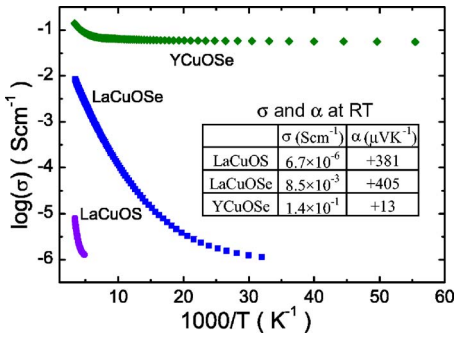

FIG. 3. (Color online) Temperature dependence of the conductivities in LnCuOCh (Ln=La,Y; Ch=S,Se). The conductivities (σ) and Seebeck coefficients (α) at room temperature are summarized in the inset.

The previous study on the electronic structure of LaCuOSe revealed that the top of the VB and the bottom of the conduction band are composed of the Cu 3*d*-Se 4*p* hybridized band and Cu 4*s*-Se 4*p* antibonding band, respectively, as illustrated in Fig. 7. In addition, the La 5*d*-O 2*p* antibonding band and O 2*p* nonbonding band are located above the Cu 4*s*-Se 4*p* antibonding band and below the Cu 3*d*-Se 4*p* hybridized band, respectively. Therefore, from the viewpoint of an electronic structure, the band gap of YCuOSe is also determined by the energy levels of the Cu 3*d*-Se 4*p* hybridized band and Cu 4*s*-Se 4*p* antibonding band, even though the Y 4*d*-O 2*p* antibonding band is located at higher energy than the La 5*d*-O 2*p* antibonding band as observed in Ln_2O_3 (Ln=La,Y).

The smaller band gap of YCuOSe than LaCuOSe is derived from its small lattice parameters due to the small ion radii of a Y ion and the band gaps of these materials are determined by the energy difference between the Cu 3*d*-Se

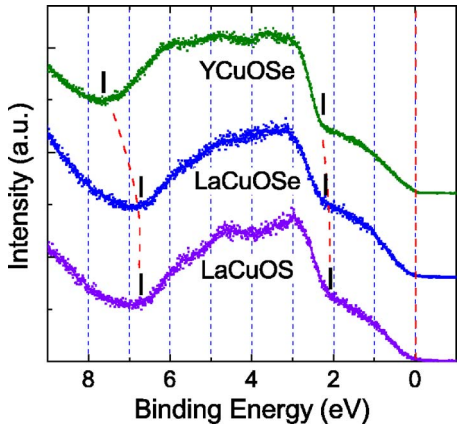

FIG. 5. (Color online) UPS (He I) spectra of LaCuOCh (Ln=La,Y; Ch =S,Se) aligned at the Fermi energy (E_b=0). The bottoms of the Cu–Se hybridized bands and the VBs are indicated by the vertical bars.

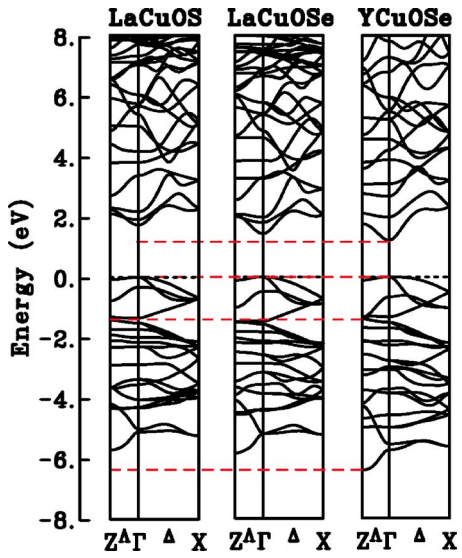

FIG. 6. (Color online) Energy band structures of LaCuOCh (Ln=La, Y; Ch=S, Se) around the Γ point. The tops of the valence band are aligned at the energy of 0 eV. Dashed lines indicate the energy levels of the bottom of the conduction band, the top and bottom of the Cu–Se hybridized band, and the bottom of the VB for YCuOSe.

4*p* hybridized band and Cu 4*s*-Se 4*p* antibonding band. However, as shown in Fig. 2, the Cu–Se distances are almost the same between YCuOSe and LaCuOSe. This fact suggests that the extent of the hybridization between Cu 3*d*-Se 4*p* orbitals is almost the same between YCuOSe and LaCuOSe without broadening the Cu 3*d*-Se 4*p* hybridized band. The UPS spectra and energy band calculations also support this idea. Since the decreases of the Ln–O and Ln–Ch distances do not influence the band gap directly, the smaller band gap and broader VB width are presumably attributed to the decrease of the Cu–Cu distances in YCuOSe. Furthermore, it is reasonable to consider that the short Cu–Cu distances increase the interaction between Cu 4*s* orbitals leading to the energy shift and broadening of the two Cu 4*s* related bands, the Cu 4*s*-Se 4*p* bonding and antibonding bands, as seen in Fig. 6 and schematically shown in Fig. 7. As a result, it is concluded that the low energy position and the broader widths of the Cu 4*s*-Se 4*p* bonding and antibonding bands are responsible for the smaller band gap and the broader VB width in YCuOSe.

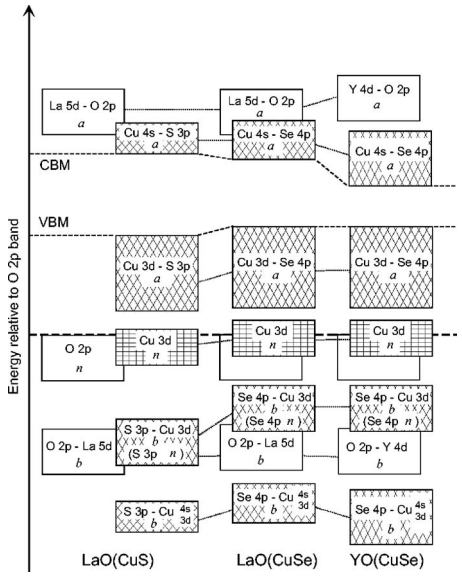

FIG. 7. Schematic band structures of LaCuOCh (Ln=La, Y; Ch=S, Se) aligned at the O 2*p* nonbonding bands. The symbols *b*, *n*, and *a* denote bonding, nonbonding, and antibonding states, respectively.

CONCLUSION

Single-phase YCuOSe samples were prepared by a solid-state reaction at 750 °C for 12 h in evacuated silica glass tubes. They showed *p*-type semiconduction, and the band gap of YCuOSe was estimated to be 2.58 eV, which is much smaller than that of LaCuOSe. The photoluminescence measurements, UPS measurements, and energy band calculations revealed that YCuOSe has a direct-type band gap and its electronic structure is basically the same with those of LaCuOCh (Ch=S and Se). In addition, the smaller band gap and larger VB width of YCuOSe were analyzed and attributed to the lowering of the energy and the broadening of the widths of the Cu 4*s* bonding and antibonding bands due to the short Cu–Cu distances and the larger Cu–Cu interactions in YCuOSe.

[1] M. Palazzi, C. R. Seances Acad. Sci., Ser. 2 **292**, 789 (1981).
[2] K. Ueda, S. Inoue, S. Hirose, H. Kawazoe, and H. Hosono, Appl. Phys. Lett. **77**, 2701 (2000); K. Ueda, S. Inoue, H. Hosono, N. Sarukura, and H. Hirano, *ibid.* **78**, 2333 (2001).
[3] K. Ueda, H. Hiramatsu, H. Ohta, M. Hirano, T. Kamiya, and H. Hosono, Phys. Rev. B **69**, 155305 (2004).
[4] H. Hiramatsu, H. Ohta, T. Suzuki, C. Honjo, Y. Ikuhara, K. Ueda, T. Kamiya, M. Hirano, and H. Hosono, Cryst. Growth Des. **4**, 301 (2004).
[5] H. Kamioka, H. Hiramatsu, H. Ohta, M. Hirano, K. Ueda, T. Kamiya, and H. Hosono, Appl. Phys. Lett. **84**, 879 (2004).
[6] Y. Takano, C. Ogawa, Y. Miyahara, H. Ozaki, and K. Sekizawa, J. Alloys Compd. **249**, 221 (1997).
[7] K. Takase, S. Kanno, R. Sasai, K. Sato, Y. Takahashi, Y. Takano, and K. Sekizawa, J. Phys. Chem. Solids **66**, 2130 (2005).
[8] K. Takase, K. Sato, O. Shoji, Y. Takahashi, Y. Takano, K. Sekizawa, Y. Kuroiwa, and M. Goto, Appl. Phys. Lett. **90**, 161916 (2007).
[9] H. Nakao, Y. Takano, K. Takase, K. Sato, S. Hara, S. Ikeda, Y. Takahashi, and K. Sekizawa, J. Alloys Compd. **408**, 104 (2006).
[10] H. Sato, H. Negishi, A. Wada, A. Ino, S. Negishi, C. Hirai, H. Namatame, M. Taniguchi, K. Takase, Y. Takahashi, T. Shimizu, Y. Takano, and K. Sekizawa, Phys. Rev. B **68**, 035112 (2003).
[11] B. A. Popovkin, A. M. Kusainova, V. A. Dolgikh, and L. G. Aksel'rud, Russ. J. Inorg. Chem. **43**, 1471 (1998).
[12] A. M. Kusainova, P. S. Berdonosov, L. G. Akselrud, L. N. Kholodkovskaya, V. A. Dolgikh, and B. A. Popovkin, J. Solid State Chem. **112**, 189 (1994).
[13] D. O. Charkin, A. V. Akopyan, and V. A. Dolgikh, Russ. J. Inorg. Chem. **44**, 833 (1999).
[14] G. H. Chan, B. Deng, M. Bertoni, J. R. Ireland, M. C. Hersam, T. O. Mason, R. P. Van Duyne, and J. A. Ibers, Inorg. Chem. **45**, 8264 (2006).
[15] W. J. Zhu, Y. Z. Huang, C. Dong, and Z. X. Zhao, Mater. Res. Bull. **29**, 143 (1994).
[16] W. J. Zhu, Y. Z. Huang, F. Wu, C. Dong, H. Chen, and Z. X. Zhao, Mater. Res. Bull. **29**, 505 (1994).
[17] A. T. Nientiedt and W. Jeitschko, Inorg. Chem. **37**, 386 (1998).
[18] D. O. Charkin, P. S. Berdonosov, V. A. Dolgikh, and P. Lightfoot, J. Alloys Compd. **292**, 118 (1999).
[19] L. Cario, H. Kabbour, and A. Meerschaut, Chem. Mater. **17**, 234 (2005).
[20] Y. Kamihara, H. Hiramatsu, M. Hirano, R. Kawamura, H. Yanagi, T. Kamiya, and H. Hosono, J. Am. Chem. Soc. **128**, 10012 (2006).
[21] H. Hiramatsu, K. Ueda, H. Ohta, T. Kamiya, M. Hirano, and H. Hosono, Appl. Phys. Lett. **87**, 211107 (2005).
[22] H. Yanagi, J. Tate, S. Park, C.-H. Park, and D. A. Keszler, Appl. Phys. Lett. **82**, 2814 (2003).

[23]K. Ueda, K. Takafuji, H. Hiramatsu, H. Ohta, T. Kamiya, M. Hirano, and H. Hosono, Chem. Mater. **15**, 3692 (2003); H. Hiramatsu, K. Ueda, K. Takafuji, H. Ohta, M. Hirano, T. Kamiya, and H. Hosono, J. Appl. Phys. **94**, 5805 (2003).
[24]K. Ueda, H. Hosono, and N. Hamada, J. Appl. Phys. **98**, 043506 (2005); K. Ueda, H. Hosono, and N. Hamada, J. Phys.: Condens. Matter **16**, 5179 (2004); S. Inoue, K. Ueda, and H. Hosono, Phys. Rev. B **64**, 245211 (2001).
[25]F. Izumi and T. Ikeda, Mater. Sci. Forum **321–324**, 198 (2000).
[26]R. D. Shannon, Acta Crystallogr., Sect. A: Cryst. Phys., Diffr., Theor. Gen. Crystallogr. **32**, 751 (1976).
[27]V. N. Abramov and A. I. Kuznetsov, Sov. Phys. Solid State **20**, 399 (1978); A. V. Prokofiev, A. I. Shelykh, and B. T. Melekh, J. Alloys Compd. **242**, 41 (1996).